Available at www.sciencedirect.com

INFORMATION PROCESSING IN AGRICULTURE 6 (2019) 233–246

journal homepage: www.elsevier.com/locate/inpa

Image based leaf segmentation and counting in rosette plants

J. Praveen Kumar, S. Domnic *

National Institute of Technology, Tiruchirappalli, India

ARTICLE INFO

Article history:
Received 23 April 2018
Received in revised form
7 August 2018
Accepted 13 September 2018
Available online 7 December 2018

Keywords:
Plant image analysis
Plant phenotyping
Leaf region extraction
Leaf count

ABSTRACT

This paper proposes an efficient method to extract the leaf region and count the number of leaves in digital plant images. The plant image analysis plays a significant role in viable and productive agriculture. It is used to record the plant growth, plant yield, chlorophyll fluorescence, plant width and tallness, leaf area, etc. frequently and accurately. Plant growth is a major character to be analyzed among these plant characters and it directly depends on the number of leaves in the plants. In this paper, a new method is presented for leaf region extraction from plant images and counting the number of leaves. The proposed method has three steps. The first step involves a new statistical based technique for image enhancement. The second step involves in the extraction of leaf region in plant image using a graph based method. The third step involves in counting the number of leaves in the plant image by applying Circular Hough Transform (CHT). The proposed work has been experimented on benchmark datasets of Leaf Segmentation Challenge (LSC). The proposed method achieves the segmentation accuracy of 95.4% and it also achieves the counting accuracy of −0.7 (DiC) and 2.3 (|DiC|) for datasets (A1, A2 and A3), which are better than the state-of-the-art methods.

1. Introduction

Plants become the essential source of food, fuel, etc. for human beings. So, the researchers and agriculture related industries with great efforts are involving in research, to continue agriculture for a prolonged period without any breach. Plant phenotyping addresses the rural requirements without any constraint. One of the important rural requirements is increasing the crop yield, which requires an exceptional amount of research. Plant phenotyping based on image analysis is used to analyse the plant traits for predicting the crop yield. Plant image analysis deals with plant measurements like growth, anatomy, shape, surface, etc. by analysing the images of different plant organs like leaves, root, etc. Various methods [1] have been proposed for controlled experimental design and particular acquisition scenarios. A few attempts have been made to create software applications [2] to analyse the plant images automatically. In achieving the goal of increasing the output of non-destructive plant phenotyping, various computer vision and imaging techniques [3] have been proposed.

A vital amount of research have been performed in the area of plant phenotyping, which includes the research in the field of plants disease identification, leaf counting, leaf segmentation, and observing the development and growth of plant by analysing the plant images. In recent days, plant phenotyping has been done in controlled laboratory environment, green house, or in the field. Many researchers

* Corresponding author.
E-mail address: domnic@nitt.edu (S. Domnic).
Peer review under responsibility of China Agricultural University.
https://doi.org/10.1016/j.inpa.2018.09.005

and academicians have contributed a lot to plant phenotyping. Huang et al. [4] proposed a method for automatic identification of plant species. Manuel Grand-Brochier et al. [5] depicted the studies to extract the tree leaves from natural images by applying various segmentation methods. Tang et al. [6] proposed an algorithm to extract the leaf region from the images with complex background. Some of the segmentation systems use infrared or depth information [7] for segmentation.

Yin et al. [8] matched the available segmented leaf templates with unseen data to segment and track the arabidopsis leaf. Dellen et al. [9] used graph-based method to track the tobacco plant leaves. De Vylder et al. [10] used the active contour method for segmenting and tracking the arabidopsis leaves. Shen et al. [11] proposed an automated system based on computer vision technology for counting the soybean leaf aphids. Cerutti et al. [12] proposed a parametric active polygon model. The drawbacks of these methods are (i) the need of prior training and large labelled datasets and (ii) the impotency of handling occlusions.

In recent times, many research works [13–16,3] have been proposed to measure the phenotypic traits. Rosette Tracker software [13] is an open source tool to evaluate the genotype effects. gPb-owt-ucm [14] is a segmentation method that depends on spectral clustering and contour detection. Maximal Similarity Based Region Merging (MSRM) [15], an interactive segmentation approach, used region merging framework for fusing the super-pixel segmentation. The drawback of these methods is either these methods result in over segmentation or under segmentation.

An et al. [16] showed the practical workflow to provide a higher image processing throughput. The phenotypic traits such as rosette area, leaf length and total leaf expansion are extracted directly from images using photogrammetry and imaging techniques. In this work, the rosette plant images are captured in a stationary growth chamber platform and a movable field platform using many cameras placed at different angles which results in color changes, occurrence of shadows and distortion in the image. Hence, they have used the preprocessing techniques such as Image color correction, Image optical distortion correction and Orthophoto generation. Subsequently, the Normalized Green–Red Difference Index (NGRDI) is used to segment the plant region from background. This extracted plant region is used to calculate the leaf length, total leaf expansion and rosette area.

The drawback of the framework proposed in [16] is that it was not generalized for all brands of cameras. It requires corresponding preprocessing software for each brand of camera. The NGRDI method is used in this framework to segment the plant region. Since, the leaf region and mosses are green in color the NGRDI method might not differentiate the leaf region from the mosses. Hence, it might lead to over segmentation.

In Simple Linear Iterative Clustering superpixels segmentation (SLIC_Seg) method [3], SLIC superpixel is used to segment the target leaf region. A superpixel [17,18] is a group of connected, perceptually homogeneous pixels, which does not overlap any other superpixel. Superpixel segmentation is dividing an image into hundreds of non-overlapping superpixels. SLIC_Seg method used superpixel over-segmentation in L*a*b colour space to extract the whole plant. Simple seeded region growing is used in the superpixel space to segment the foreground. Training is not required for this method.

In leaf segmentation with Chamfer matching (Chamfer_Seg) method [3], segmentation and tracking of the leaves were originally applied in plant fluorescence videos. In this method, a set of templates with different scales, shapes, and orientations was generated and matched to find the individual leaves. Leaf segmentation by watershed (Watershed_Seg) method [3] comprises two phases: In the first phase, supervised classification and neural network were used to segment foreground from the background. In the second stage, the watershed method was applied on euclidean distance map of the resulting plant mask from the plant segmentation phase to identify the individual leaves.

There are few limitations in these methods. In Chamfer_Seg method, the accuracy of leaf extraction depended on the number of templates created. In this method, if the plant images consist of leaves with huge difference in shape and size, there was a need to create more templates. Therefore, template creation became a difficult task. And also, the hourly throughput of this method was less compared to other methods, which was a major drawback of this method. In Watershed_Seg method, the dataset had to be trained initially. The performance of the system was based on the initial training. The ground truth images were used to mask plant and background pixels. Since Watershed_Seg method relied on ground truth images, it might not be used in cross platform. In SLIC_Seg method, the segmentation accuracy directly depended on the superpixels selection. Moreover, the Watershed_Seg and SLIC_Seg methods did not perform equally well for all the images in the datasets and hence, not maintaining the robustness of the system.

Based on the related works, it is concluded that the performance of the existing works depends on the preprocessing software for image enhancement and training datasets or templates for plant region segmentation. To overcome the drawbacks of these systems, a new method is developed which includes statistical based image enhancement, graph based leaf region extraction and CHT based leaf counting. The contributions of the proposed work are: (i) the statistical properties of an image are studied to automatically identify whether the image needs to be preprocessed and the illumination effect is removed using proposed statistical based image enhancement technique. (ii) the graph based method is proposed for leaf region segmentation and the number of leaves is counted using Circular Hough Transform (CHT). The main advantages of the proposed method are: (i) training is not required, (ii) independent of device and preprocessing software, (iii) automatically identifies whether the image needs to be enhanced based on the statistical properties of the image and (iv) applicable in various phenotyping platforms and environments with minimal modification.

2. Materials and methods

2.1. *Dataset description and evaluation criteria*

The datasets (A1, A2 and A3) are the benchmark datasets [1], which are used for evaluating the proposed work. A1, A2 and

A3 consist of plant images arranged in trays that are used for Leaf segmentation challenge. The datasets A1 and A2 comprise top-view and time-lapse images of Arabidopsis arranged in trays, which are captured using a 7 MP Canon Power-Shot SD1000 camera. A3 dataset consists of tobacco plant images which are captured using Grashopper cameras. A1 dataset images are captured for 3 weeks once in every 6 h during day time. A2 dataset images are captured for 7 weeks once in every 20 min during day time. The acquired raw images are encoded using lossless compression standard existing in the PNG file format.

A1 dataset consists of 128 (500 × 530 pixels) images with changing and complex background. A2 dataset have 31 (530 × 565 pixels) images with simpler scene. A3 dataset have 27 (2448 × 2048 pixels) images with high resolution. The different mutants of plant images at different growth stages are included in the datasets (A1, A2 and A3). The datasets consist of images of group of plants and isolated plants. The plant images in the datasets vary in fidelity, scene complexity and resolution. Due to varying scene complexities and the presence of plant objects, there are many challenges in the datasets with respect to analysis. Images having many challenging situations are included in the datasets. In A1 and A2, there are presence reflections due to irrigation water in the tray. Overlapping of leaves occur, when the plant grows, and result in leaf occlusions. From time to time, there are changes in shapes and sizes due to nasty movements of leaves. In A3, the leaf shapes are different due to various treatments apart from changes due to nasty movement. High and low illumination condition is one of the treatments. Leaves become round and large under low illumination condition. Plants become more compact due to overlapping and partly wrinkled leaves under high illumination condition.

In A1 dataset, the Arabidopsis images with changing and complex background produce more impediments in leaf region extraction. The changing and complex background scene includes the presence of external objects like markers or tape and slightly focuses out of the scene in a few images. The presence of yellowish dry soil and mosses on the soil in certain pots also increase the complexity of leaf region extraction. The A2 dataset images show simpler scene with more uniform background, sharper focus and without mosses on the soil. However, the A2 dataset has plant images of various phenotypes mutants of Arabidopsis related to rosette plant with different leaf sizes and shape. A3 dataset possess tobacco images with high resolution. These images produce more computational complexity. The factors like leaf hairs, leaf colour variation, self-occlusion and shadows make the scene even more complex.

The authors in the existing works have used different metrics for evaluating their works. They are (i) Foreground–Background Dice (FBD%): used to evaluate delineation of extracted plant region with respect to ground truth, (ii) Difference in Count (DiC): used to find the difference between the number of leaves in extracted leaf region and the ground truth, (iii) Absolute value of DiC (|DiC|),(iv) Dice score (Dice%), which is given in Eq. (1) used to measure the spatial overlap between the extracted leaf region and the ground truth, (v) Precision, which is given in Eq. (2) used to determine the portion of extracted leaf region pixels that matches with the ground truth, (vi) Recall, as given in Eq. (3), used to find how much portion of ground-truth pixels present in the extracted leaf region and (vii) Jaccard, as given in Eq. (4), used to determine the spatial overlap between the extracted leaf region and the ground truth.

$$Dice\ (\%) = ((2 \times TP) \div ((2 \times TP) + FP + FN)) \times 100 \quad (1)$$

$$Precision\ (\%) = (TP \div (TP + FP)) \times 100 \quad (2)$$

$$Recall\ (\%) = (TP \div (TP + FN)) \times 100 \quad (3)$$

$$Jaccard\ (\%) = (TP \div (TP + FP + FN)) \times 100 \quad (4)$$

where True Positive (TP), False Negative (FN) and False Positive (FP) represent the number of leaf region pixels correctly identified, the number of leaf region pixels unidentified and the number of leaf region pixels falsely identified respectively.

In paper [3], the metric FBD% is used to measure the accuracy of extracted leaf region and DiC is used to find the accuracy of counting the leaves. The metrics such as Dice, Precision, Recall and Jaccard are used by the authors in their research works [13,14] to measure the segmentation accuracy. Since different metrics have been used by different authors to measure the segmentation accuracy, all these metrics are used to evaluate the performance of the proposed method.

The proposed method is implemented using Matlab (release 2016), on a system with Intel i3 processor 2.66 GHz speed and 4 GB memory, running on 64 bit windows operating system. The proposed method is tested with LSC benchmark datasets A1, A2, A3 and whole tray plant images under several challenging situations such as moss growth and reflection of light. On an average, the processing time of each image in A1 and A2 datasets takes approximately 2 s and approximately 10 s for each image in A3 dataset. Therefore, the hourly throughput is approximately 1800 plants per hour for A1 and A2 datasets and approximately 360 plants per hour for A3 dataset.

2.2. Proposed method

The proposed graph based model in this paper has been designed to extract the leaves from the given plant images with minimum manual interaction. The proposed methodology is shown in Fig. 1. It consists of three steps: Image enhancement, Leaf extraction and Leaf counting.

In the proposed method, the statistical model for illumination effect removal, the graph model for leaf extraction and the CHT for leaf counting have been adopted.

2.2.1. Image enhancement

The natural plant images may contain shadows or illumination effect, which depends on the brightness of the image. The presence of shadow or illumination effect affects the performance of leaf region identification. The brightness of an image is represented by the V plane [19] of its corresponding HSV image. This effect caused by the changes in brightness can be reduced by pre-processing the V plane of HSV colour space. Image enhancement is the technique used to enhance the illumination effect. The illumination of an image is the range of values for brightness in an image. By applying image enhancement technique, the features of an image will be

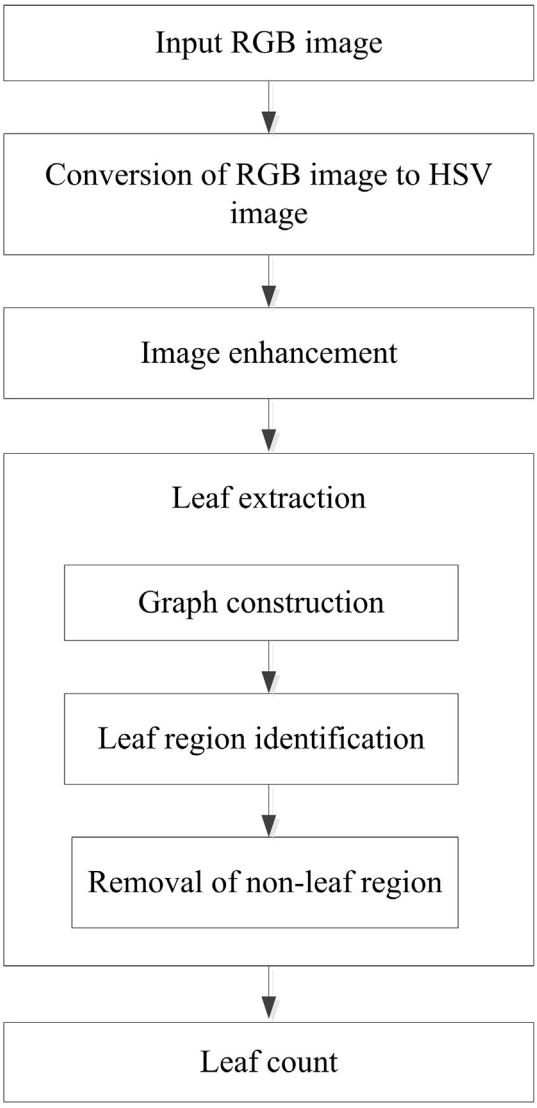

Fig. 1 – Process of extracting the leaf region and counting the leaves.

clearly identified [20]. In the proposed work, initially the RGB image of the plant is converted to HSV image. The image enhancement is carried out in the V plane of HSV image since, it corresponds to the brightness of the image. Let the pixels in the V plane are represented as $\{x_{11}, x_{12}, \cdots, x_{mn}\}$, where m and n are the number of rows and columns of the V plane respectively. The skewness (S_k) (given in Eq. (5)) and the probability distribution of V plane are calculated.

$$S_k = (E(x_{ij} - \mu)^3)/\sigma^3 \quad (5)$$

where x_{ij} denotes the value of $(i,j)^{th}$ pixel in V plane of HSV image before image enhancement, E denotes the expected value, μ denotes the mean value and σ denotes the standard deviation.

If the skewness (S_k) of the V plane is positive or negative, the enhancement of V plane is required to remove the illumination effect. When there is shadow in the image, the skewness will be positive (i.e) the distribution is converged to the left. When there is over brightness in the image, skewness will be negative (i.e) the distribution is converged to the right. In statistical modelling of contrast enhancement [21], the statistical properties of an image can be analytically calculated by probability distribution function of an image. The probability distribution is a function which gives all the possible values and likelihoods of a random variable within a range. In the proposed work, the distribution of brightness (V plane) is assumed to be in Weibull distribution. The probability density function (pdf) of Weibull distribution [22] for an image is given by

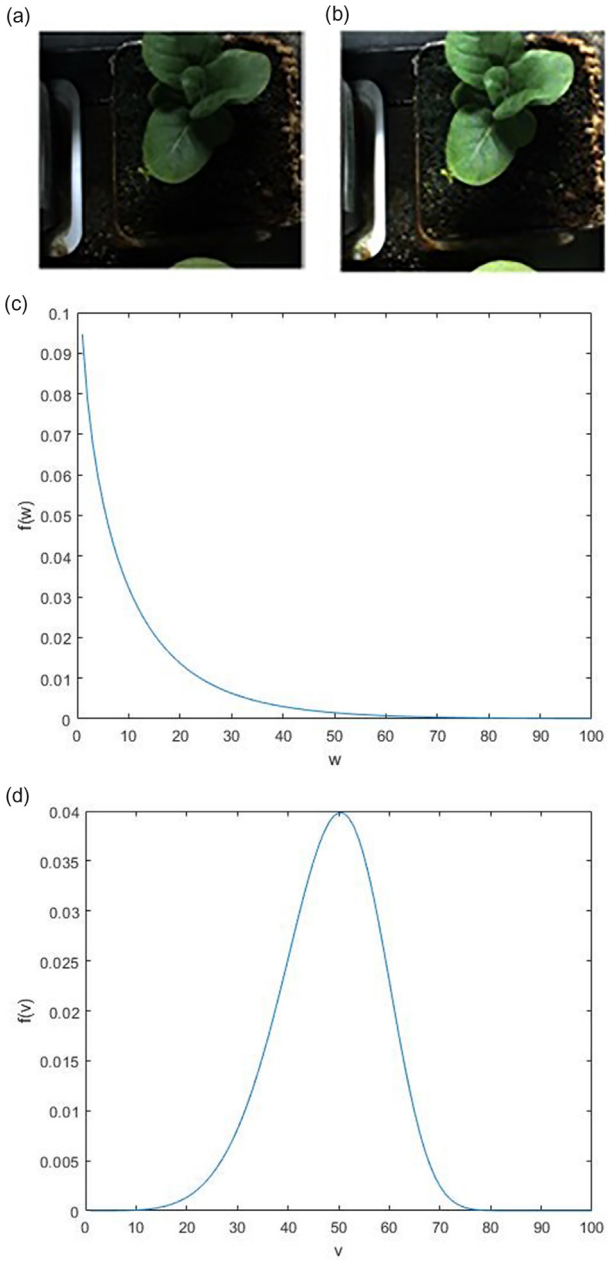

Fig. 2 – Effect of image enhancement. (a) Original image, (b) Enhanced image, (c) Brightness (V) distribution function before enhancement, (d) Brightness (V) distribution function after enhancement.

$$w_{ij} = f(x_{ij}|a,b) = \frac{b}{a}\left(\frac{x_{ij}}{a}\right)^{b-1} e^{-\left(\frac{x_{ij}}{a}\right)^{b}} \quad (6)$$

where x_{ij} and w_{ij} denote the value of $(i,j)^{th}$ pixel in V plane of HSV image, before and after applying Weibull distribution respectively, 'a' denotes the scale parameter and 'b' denotes the shape parameter.

In order to remove the over brightness or shadow effect in the image, the skewness of the brightness distribution should be made symmetric as shown in Fig. 2. The brightness distribution becomes symmetric, when its values are spread out. The scale parameter is responsible to spread or compress the brightness distribution. In our experimentation, the value of scale parameter (a) is set to the mid-value of normalized V plane and the value of shape parameter (b) is set to any positive value. Using these parameters, the Weibull distribution is applied over V plane. Now, the new values of V plane are represented as $w_{i,j}$. The mean value (μ_v) of $w_{i,j}$ is calculated which is given in Eq. (7). Then, the intensity transformation function as given in Eq. (8) is used to spread the brightness distribution.

$$\mu_v = mean(w_{i,j}) \quad (7)$$

$$v_{i,j} = T(w_{i,j}) = \begin{cases} \mu_v, & w_{i,j} < \mu_v \wedge S_k > 0 \\ \mu_v, & w_{i,j} > \mu_v \wedge S_k < 0 \\ w_{i,j}, & otherwise \end{cases} \quad (8)$$

where T is the transformation function, $w_{i,j}$ and $v_{i,j}$ are the values of $(i,j)^{th}$ pixel in V plane, before and after the image enhancement respectively.

After applying Eq. (8) on V plane, the image will be enhanced by removing the shadow or illumination effect, which in turn improves the segmentation accuracy.

2.2.2. *Leaf extraction*

The enhanced HSV image obtained as the result of image enhancement phase is given as input to this phase. In the

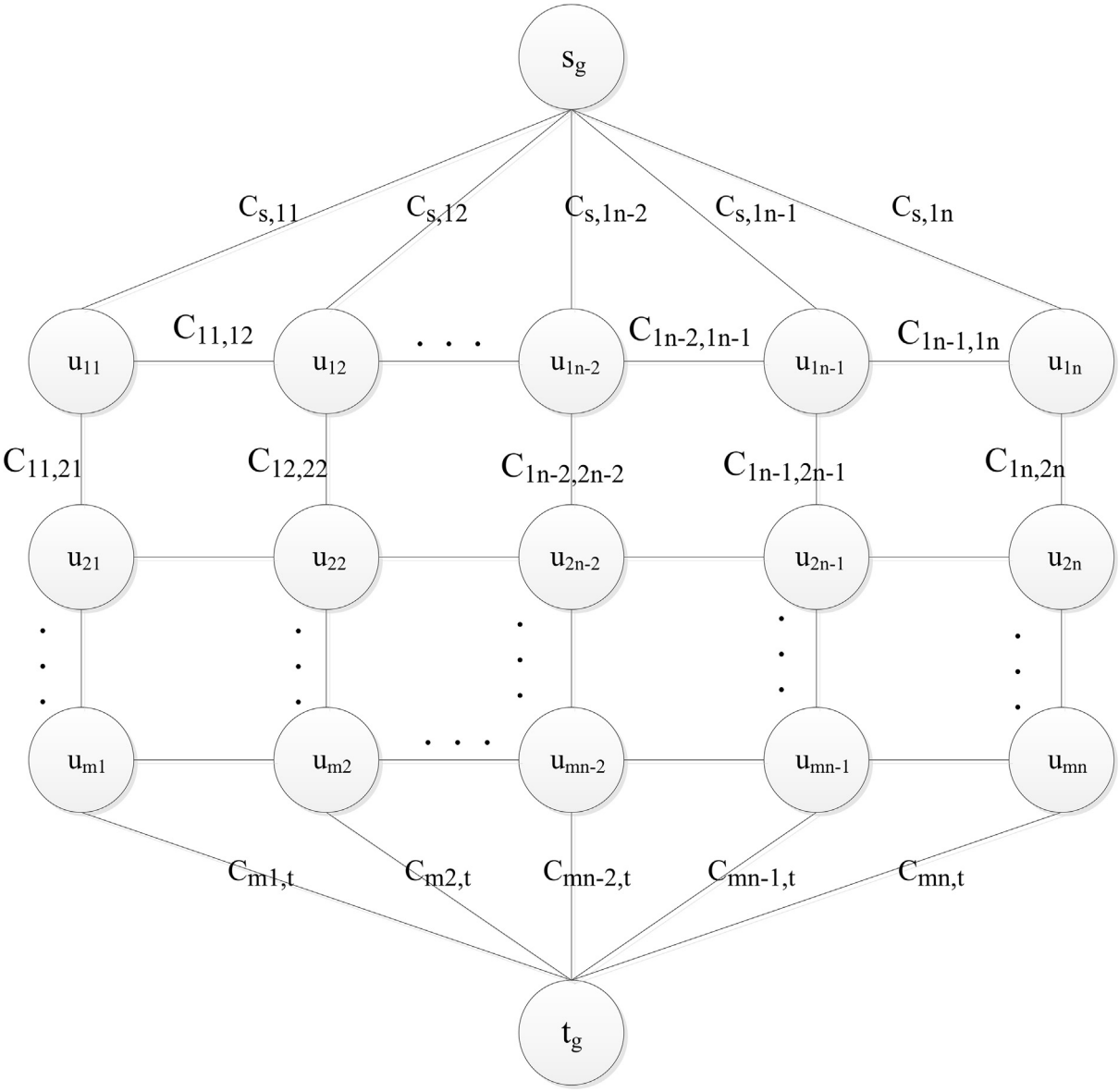

Fig. 3 – Graph construction for leaf region identification.

enhanced HSV image, the pixels of V plane only are changed and other two planes (H and S) remain unchanged. The proposed method uses graph based algorithm to segment the leaf region, which increases the segmentation accuracy by maintaining the robustness to reflections and shadows. The complexity of the proposed leaf segmentation algorithm is O(m × n), where m and n are the number of rows and columns of the image respectively. There are three phases in the leaf extraction step. They are (a) Graph construction (b) Leaf region identification (c) Removal of non-leaf region.

2.2.2.1. Graph construction. The graph is constructed based on enhanced HSV image, which is used for leaf region segmentation. For an enhanced HSV image, the graph G_r = (U, E) is constructed as shown in Fig. 3. The nodes $\{u_{11}, u_{12}, \cdots, u_{mn}\} \in U$ represent the pixels of the enhanced HSV image, where m and n are the number of rows and columns of the enhanced HSV image respectively and $(u_{ij},u_{ij+1}) \in E$ denotes the edge connecting the pixels u_{ij} and u_{ij+1}, where $i = 1, 2, \ldots, m$ and $j = 1, 2, \ldots, n$. The graph construction procedure starts with the node u_{11}, which represents the first pixel of the enhanced HSV image and ends with the node u_{mn} (i.e) the last pixel of the enhanced HSV image. The edges in the graph can be classified into two types: (i) edge between pair of neighbouring pixels and (ii) edge between a pixel and source or terminal. The relationship between the pixels of the HSV image is given by the edge weight or edge cost. Each edge in the graph is assigned to an edge cost. In order to segment the leaf region, $C_{s,ij}$ (the edge cost between source node s_g and the pixel u_{ij}), $C_{ij,ij+1}$ (the edge cost between the two

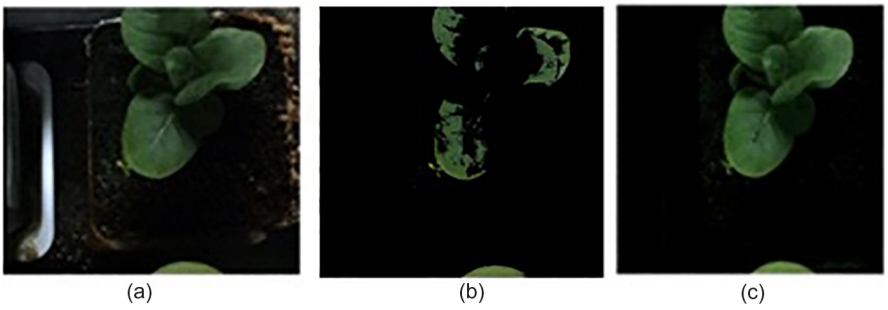

Fig. 4 – Leaf region extraction of plant image illustrating the importance of image enhancement. (a) Original image, (b) Extracted image without enhancement, (c) Extracted image with enhancement.

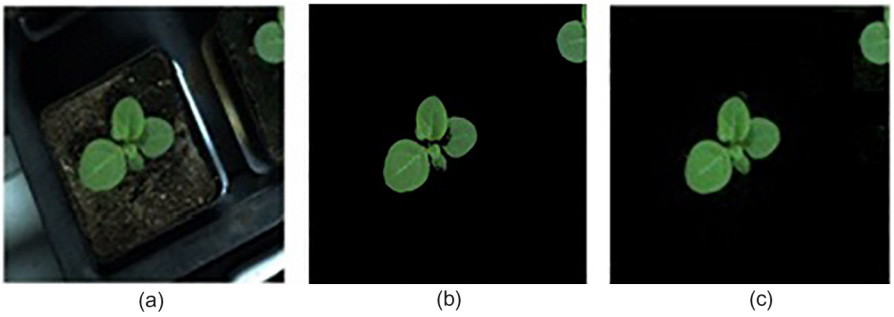

Fig. 5 – Leaf region extraction of plant image illustrating the importance of image enhancement. (a) Original image, (b) Extracted image without enhancement, (c) Extracted image with enhancement.

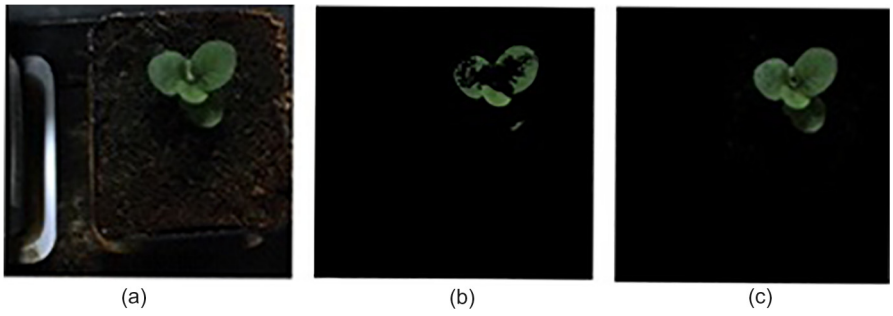

Fig. 6 – Leaf region extraction of plant image illustrating the importance of image enhancement. (a) Original image, (b) Extracted image without enhancement, (c) Extracted image with enhancement.

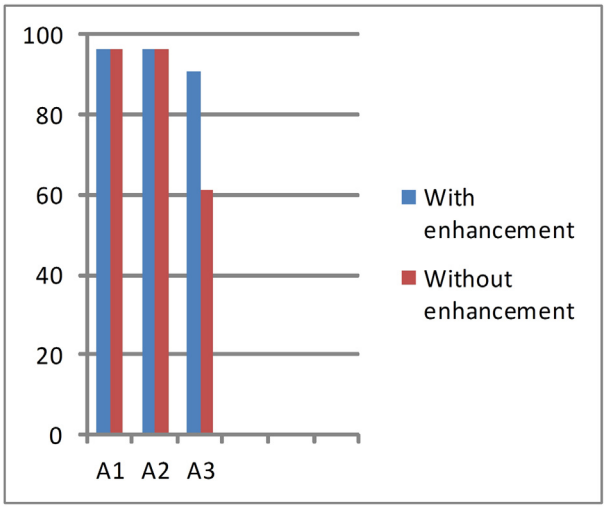

Fig. 7 – The Dataset-FBD% graph obtained for performance comparison of proposed method with image enhancement and without image enhancement.

neighbouring pixels u_{ij} and u_{ij+1}) and $C_{ij,t}$ (the edge cost between the pixel u_{ij} and terminal node t_g)) can be calculated as follows:

Let the parameters used to find the edge cost prediction parameter (given in Eq. (12)) be defined by

$$\theta_H = \{u_H : \tau_{min\_H} \le H(u_{ij}) \le \tau_{max\_H}\} \tag{9}$$

$$\theta_S = \{u_S : \tau_{min\_S} \le S(u_{ij}) \le \tau_{max\_S}\} \tag{10}$$

$$\theta_V = \{u_V : \tau_{min\_V} \le V(u_{ij}) \le \tau_{max\_V}\} \tag{11}$$

where $H(u_{ij})$, $S(u_{ij})$ and $V(u_{ij})$ are the values of pixel u_{ij} in 'H' plane, 'S' plane and 'V' plane of enhanced HSV image respectively. The values of these parameters are $\tau_{min\_H} = 0.17$, $\tau_{max\_H} = 0.4$, $\tau_{min\_S} = 0.2$, $\tau_{max\_S} = 1$, $\tau_{min\_V} = \mu_v$ and $\tau_{max\_V} = 1$ where μ_v is calculated using Eq. (3). These parameters values are chosen experimentally and are commonly used for datasets A1, A2, and A3.

$$P_{ij} = \begin{cases} true, & if\ H(u_{ij}) \in \theta_H \wedge S(u_{ij}) \in \theta_S \wedge V(u_{ij}) \in \theta_V \\ false, & otherwise \end{cases} \tag{12}$$

where P_{ij} is the edge cost/edge weight prediction parameter.

The P_{ij} is used to predict the relationship among pixels, which are represented as edge costs in the graph. In the proposed work, the edge costs are calculated as follows.

$$C_{s,ij} = \begin{cases} 0, & if\ P_{ij}\ is\ true \\ 1, & otherwise \end{cases} \tag{13}$$

where $C_{s,ij}$ is the edge cost between source node s_g and the pixel u_{ij}.

$$C_{ij,ij+1} = \begin{cases} 0, & if\ P_{ij} \wedge P_{ij+1}\ is\ true \\ 1, & otherwise \end{cases} \tag{14}$$

where $C_{ij,ij+1}$ is the edge cost between the pixels u_{ij} and u_{ij+1}, P_{ij} and P_{ij+1} are the edge cost prediction parameters for neighbouring pixels u_{ij} and u_{ij+1} respectively.

$$C_{ij,t} = \begin{cases} 1, & if\ P_{ij}\ is\ true \\ 0, & otherwise \end{cases} \tag{15}$$

where $C_{ij,t}$ is the edge cost between the pixel u_{ij} and terminal node t_g.

Eqs. (9)–(15) are used to construct the graph for segmenting the leaf region of the given plant image.

2.2.2.2. Leaf region identification:. Once the graph for the input plant image is constructed (as shown in Fig. 3), the proposed graph based algorithm (Algorithm 1) is used to segment the leaf region from the background. In the proposed algorithm, the path starting from the source node (s_g) is found to segment the leaf region. To find the path, two different

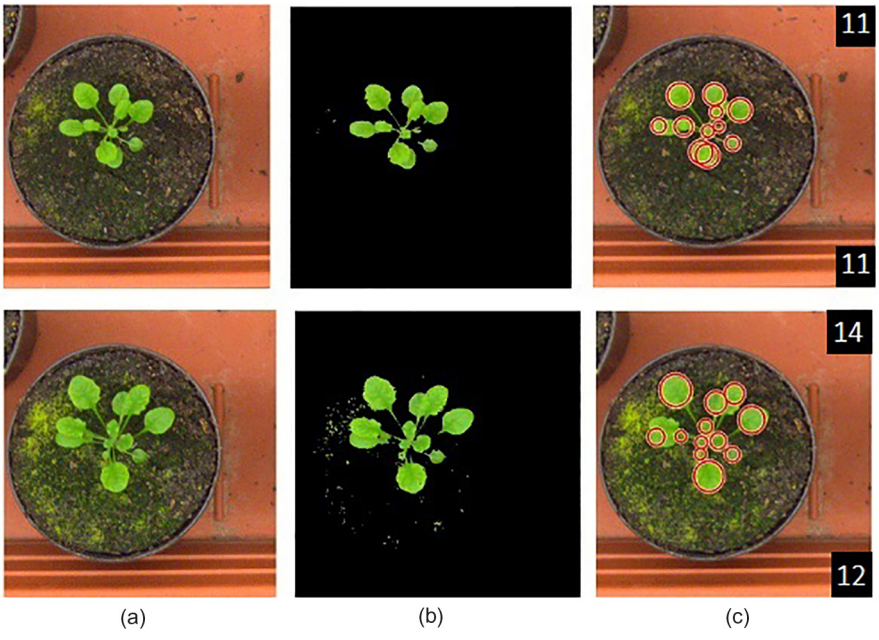

Fig. 8 – Identification of Leaves in plant images from dataset A1. (a) Original image, (b) Extracted leaf region, (c) Leaf count (Actual leaf count at right top and Identified leaf count at right bottom).

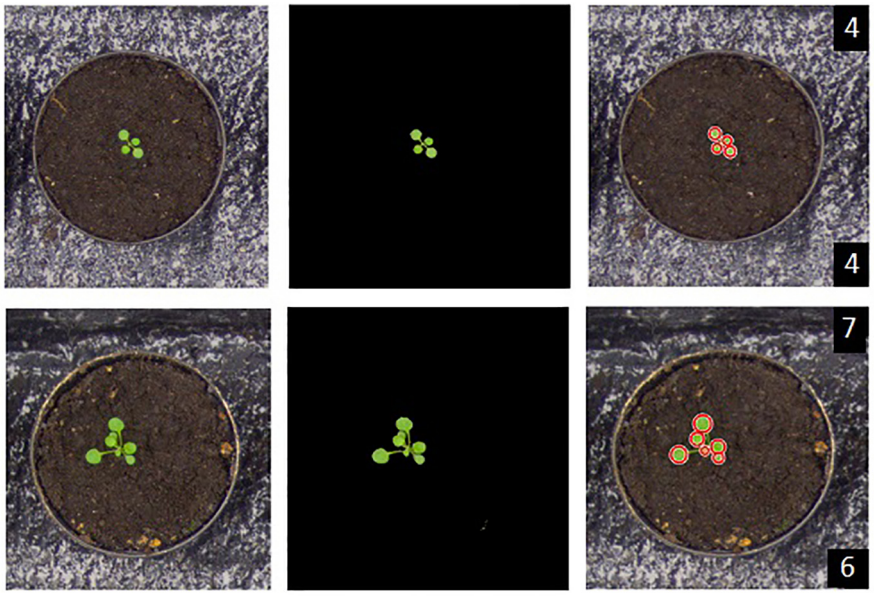

Fig. 9 – Identification of Leaves in plant images from dataset A2. (a) Original image, (b) Extracted leaf region, (c) Leaf count (Actual leaf count at right top and Identified leaf count at right bottom).

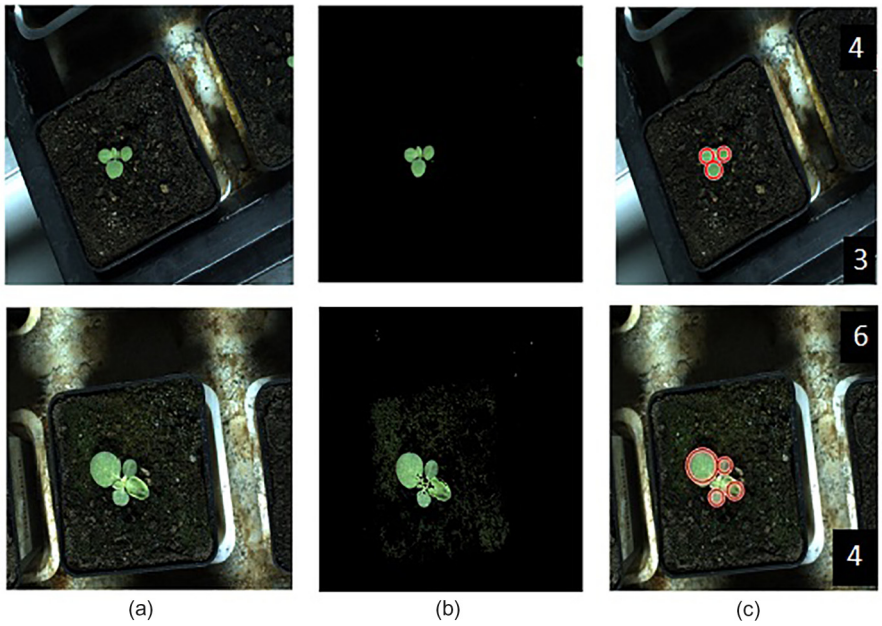

Fig. 10 – Identification of Leaves in plant images from dataset A3. (a) Original image, (b) Extracted leaf region, (c) Leaf count (Actual leaf count at right top and Identified leaf count at right bottom).

Table 1 – Performance variation in proposed system to show the contribution of image enhancement.

System	FBD %			
	A1	A2	A3	Overall
Proposed method without image enhancement	96.2	96.2	61.1	91.1
Proposed method with image enhancement	96.2	96.2	90.8	95.4

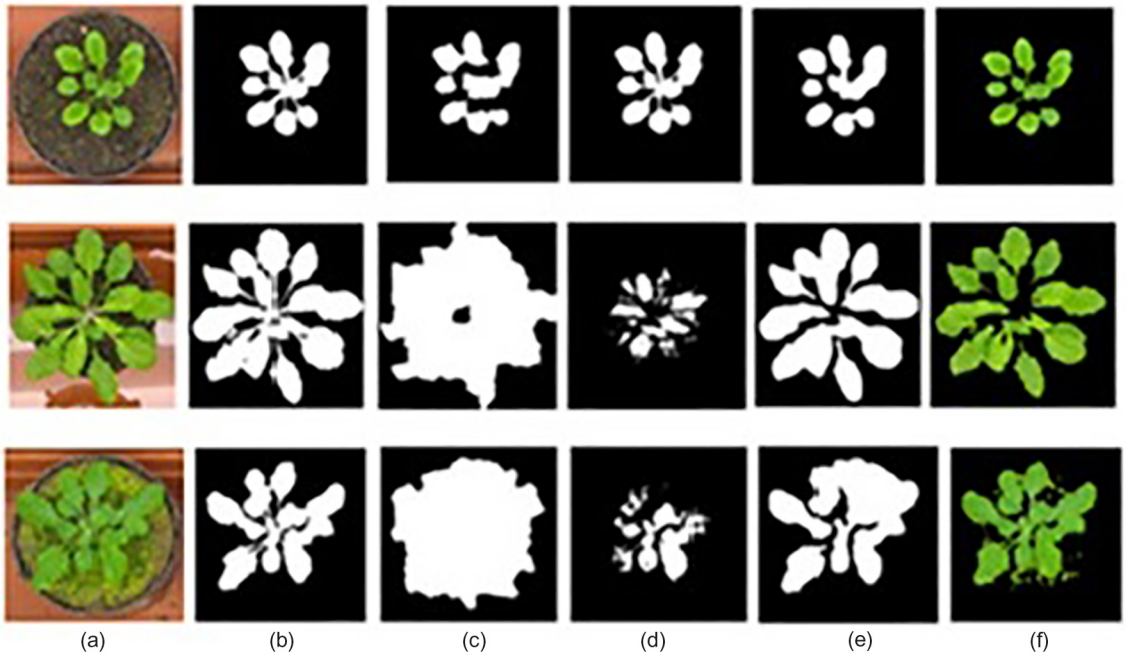

Fig. 11 – Leaf region extraction of individual plant images using various methods. (a) Original image, (b) Ground truth, (c) CoSand (2011), (d) SDSP (2013), (e) gPb-owt-ucm (2011), (f) Proposed method.

Table 2 – Performance comparison of leaf region extraction results for tray plant images.

Method/tool	Accuracy (%)			
	Precision	Recall	Jaccard	Dice
gPb-owt-ucm (2011)	89.04 (6.40)	96.20 (2.78)	85.86 (5.49)	92.29 (3.36)
Rosette Tracker (2012)	88.86 (6.49)	78.83 (24.37)	71.20 (22.29)	80.37 (22.57)
Proposed	96.48 (1.40)	91.48 (2.52)	88.48 (1.39)	**93.88 (0.79)**

Table 3 – Performance comparisons of leaf region extraction and leaf counting results for A1, A2 and A3 datasets.

Dataset	SLIC_Seg (2016)			Proposed method		
	FBD %	|DiC|	DiC	FBD %	|DiC|	DiC
A1	94.6 (1.6)	3.8 (2.0)	−3.6 (2.4)	96.2 (1.9)	2.0 (1.8)	−0.9 (2.5)
A2	87.5 (19.7)	2.5 (1.5)	−2.5 (1.5)	96.2 (2.4)	3.8 (4.7)	1.2 (5.9)
A3	79.4 (34.5)	2.3 (1.8)	−2.3 (1.9)	90.8 (6.3)	1.8 (0.9)	−1.8 (0.9)
ALL	91.2 (16.2)	3.4 (2.0)	−3.2 (2.2)	**95.4** (3.5)	**2.3** (2.5)	**−0.7** (3.3)

search trees (S_tree and T_tree) one from the source node and the other from the terminal node are built. These trees are reused to segment the leaf region and non-leaf region such that it avoids in finding the path starting from source node or terminal node, when there is a presence of neighboring edges connecting the internal nodes (except source and terminal) having equivalent weights.

Initially, all the nodes in the graph are considered to be unvisited and the search trees S_tree and T_tree are empty. The initial node for the search tree S_tree is selected from the unvisited nodes based on the Eqs. (9)–(11). Now, this selected node becomes a "leaf_margin" node for S_tree. Then, the neighbor edges of this "leaf_margin" node are explored and if the edge cost is zero, the particular neighbor node is added to S_tree, otherwise it will be added to T_tree and that particular neighbor node is considered as visited node. If a new node is added to S_tree, the "leaf_margin" node becomes a "leaf_non_-margin" node and the new node which is added to S_tree will become the "leaf_margin" node. Now, the unexplored neighbor edges of the "leaf_margin" node are explored. The edge cost of recently explored edge of "leaf_margin" node is added with the edge cost of the unexplored neighbor edges of "leaf_margin" node and makes the unexplored neighbor nodes to "leaf_margin" nodes of the S_tree, if the total edge cost is zero. Otherwise, the corresponding unexplored neighbor nodes to "leaf_margin" nodes are added to T_tree. As soon as all neigh-

bor nodes of a given "leaf_margin" node are explored and if at least one neighbor node is added to the search tree S, the leaf_margin node becomes "leaf_non_margin" node and newly added node becomes "leaf_margin" node.

Similar to S_tree, the search tree T_tree has two types of nodes: "non_leaf_margin" nodes and "non_leaf_non_margin" nodes, which correspond to the non-leaf region boundary and the internal non_leaf region respectively. A path is found, when a leaf_margin node in search tree S_tree detects a neighbor node that belongs to the search tree T_tree. The nodes in search tree S_tree and T_tree correspond to the leaf region and the non-leaf region respectively. The algorithm converges when all the nodes in the graph are added to either S_tree or T_tree. The algorithm1 describes the graph based leaf region segmentation.

Algorithm 1. Graph based leaf region segmentation

1: Input: Constructed Graph G_r
2: s_g = Source_node
3: t_g = Terminal_node
4: u_{ij} = intermediate node
5: LM = Leaf_margin node
6: LNM = Leaf_non_margin node
7: $C_{s,ij}$ = edge cost/weight between the source node and u_{ij} (p).
8: $C_{LM,q}$ = edge cost/weight between LM and the neighbor node (q) of u_{ij}.
9: nq = non visited nearest Leaf region node
10: $C_{L,q}$ = edge cost/weight between nq and its non_visited neighbor node.
11: S_tree = Search tree corresponding to leaf region
12: T_tree = Search tree corresponding to non-leaf region
13: Initialize: S_tree = {}, T_tree = {}, Unvisited = {u_{11}, u_{12}, . . ., u_{mn}}.
14: Choose a Leaf region node u_{ij} (p) from Unvisited such that $C_{s,ij} = 0$
15: $LM = p$.
16: Unvisited = Unvisited − {p}
17: **While** (Unvisited ≠ ∅)
18: **For** every neighbor node (q) of LM
19: **if** q is already visited
20: $C_{LM,q} = C_{L,nq}$; $LM = q$; $q = nq$.
21: **end if**
22: $C_{LM,q} = C_{LM,q}$ + edge cost of recently explored edge of LM.
23: **if** $C_{LM,q} = 0$
24: Add the node q to S_tree.
25: $LNM = LM$
26: $LM = q$.
27: Unvisited = Unvisited − {q}
28: **else**
29: $C_{LM,q} = 0$
30: Add the node q to T_tree.
31: Unvisited = Unvisited − {q}
32: **end if**
33: **end for**
34: **end while**
35: **end procedure**

2.2.2.3. Removal of non-leaf region. The leaf regions identified in enhanced HSV image may have few non-leaf regions such as reflection of light, yellow soil and mosses. The leaf region identified in enhanced HSV image is converted into RGB image. In order to remove the non-leaf regions, this RGB image is converted to CMYK and L*a*b colour spaces. CMYK colour space differentiates the leaf region from the reflection of light and yellow soil. The *a plane of L*a*b colour space differentiates the leaf region from the mosses. By setting threshold values for various planes of these colour spaces, the yellow soil, reflection of light and mosses can be removed from the identified leaf region image. The threshold value for C, M, Y, K and *a colour spaces are set to 85, 15, 180, 110 and 108 respectively for dataset A1; 0.25, 0.25, 0.6, 0.75 and 10 respectively for dataset A2 and 0.35, 0.2, 0.45, 0.4 and 10 respectively for dataset A3. These threshold values are chosen experimentally. The leaf region obtained as a result of this phase is used in leaf counting phase.

2.2.3. Leaf count

This phase involves in counting the total number of leaves in the extracted leaf region. The Circular Hough Transform (CHT) [23–26] is used to count the Arabidopsis leaves, since they are mostly round in nature. In CHT, the circular patterns of the image are detected. The curves corresponding to the points that are collinear intersect at the common point. The characteristics of the lines passing through these points are given by the intersection point. This shows that the obtaining concurrent curves involve in identifying the collinear points. Therefore, CHT can be treated as the modified Hough Transform. The Circular Hough Transform involves in transforming the feature points of the image space to accumulated votes of the parameter space. Then, for all parameter combinations and each feature point, the votes are gathered in an accumulator array (3D_Hough_Array (h_0, k_0, r)). The array elements having the larger number of votes denote the presence of circle.

CHT involves two steps: (i) Finding the center of the circle (c) (ii) Finding the radius of the circle (r). The center of the circle can be identified by the limitation that the normal vectors to the circular boundary intersect at the center of the circle. The normal vectors (n_1, n_2, . . .,n_n) can be identified by using edge detection operators [23]. The radius of the circle can be found by using histogram technique for $\delta = (x - h_0)^2 + (y - k_0)^2$, where ($h_0$, k_0) is the center (c) of the circle, which is identified in the first step of the CHT. The highest peak in the histogram δ acts as the radius of the circular region.

The extracted leaf region obtained from the leaf extraction phase is given as input to the leaf counting phase. The Circular Hough Transform is applied over this leaf region. The individual leaves are identified and counted based on the circular region in the leaves. The number of center of the circle gives the total number of leaves in the plant image.

The following steps are used to count the leaves in the plant image.

Step-1: Convert the extracted leaf image to grayscale image.

Step-2: Apply edge detection operator (Canny [27]) on grayscale image to detect the leaf edges and the normal vectors to leaf edges.
Step-3: c(h_0, k_0) ← intersecting point of large number of normal vectors.
Step-4: Find the histogram for $\delta = (x - h_0)^2 + (y - k_0)^2$
Step-5: r ← peak _histogram ($\delta = (x - h_0)^2 + (y - k_0)^2$)
Step-6: Create 3 dimensional Hough array 3D_Hough_Array (h_0, k_0, r).
Step-7: For each pixel in leaf image
If (pixel = edge_pixel) then
Increment the elements in 3D_Hough_Array (h_0, k_0, r) corresponding to that pixel.
Endif
Endfor
Step-8: Collect all candidate circles and delete the similar ones.
Step-9: Draw circles around the circular leaf region.
Step-10: Leaf count ← count(c(h_0, k_0)).

As a result of leaf extraction and leaf counting steps, the leaf regions are automatically extracted and the total number of leaves is counted in plant images with minimal user interaction.

3. Results and discussion

The proposed method is experimented with image enhancement technique and also without image enhancement technique for all datasets (A1, A2 and A3). The figures (Figs. 4–6) show the importance of image enhancement. The figures (Figs. 8–10) show the experimental results on plant images with varying complexities. Table 1 shows the performance of proposed work with enhancement of V plane and without enhancement of V plane.

Fig. 7 shows the importance of image enhancement. The advantage of the proposed method is it can be deployed on different phenotyping platforms in multiple environments with minimal modification in noise removal stage. The proposed method is compared with state-of-the-art methods of plant phenotyping [14,28,29]. Fig. 11 shows the comparison of leaf region extraction results of the proposed method with these algorithms. Table 2 shows the comparison of leaf region extraction performance of the proposed method with the Rosette Tracker tool [13] and Hierarchical Image Segmentation (gPb-owt-ucm) method [14]. The performance of the proposed method is also compared with the recent relevant method SLIC_Seg [3] as shown in Table 3. The segmentation and leaf counting performance of the proposed method is

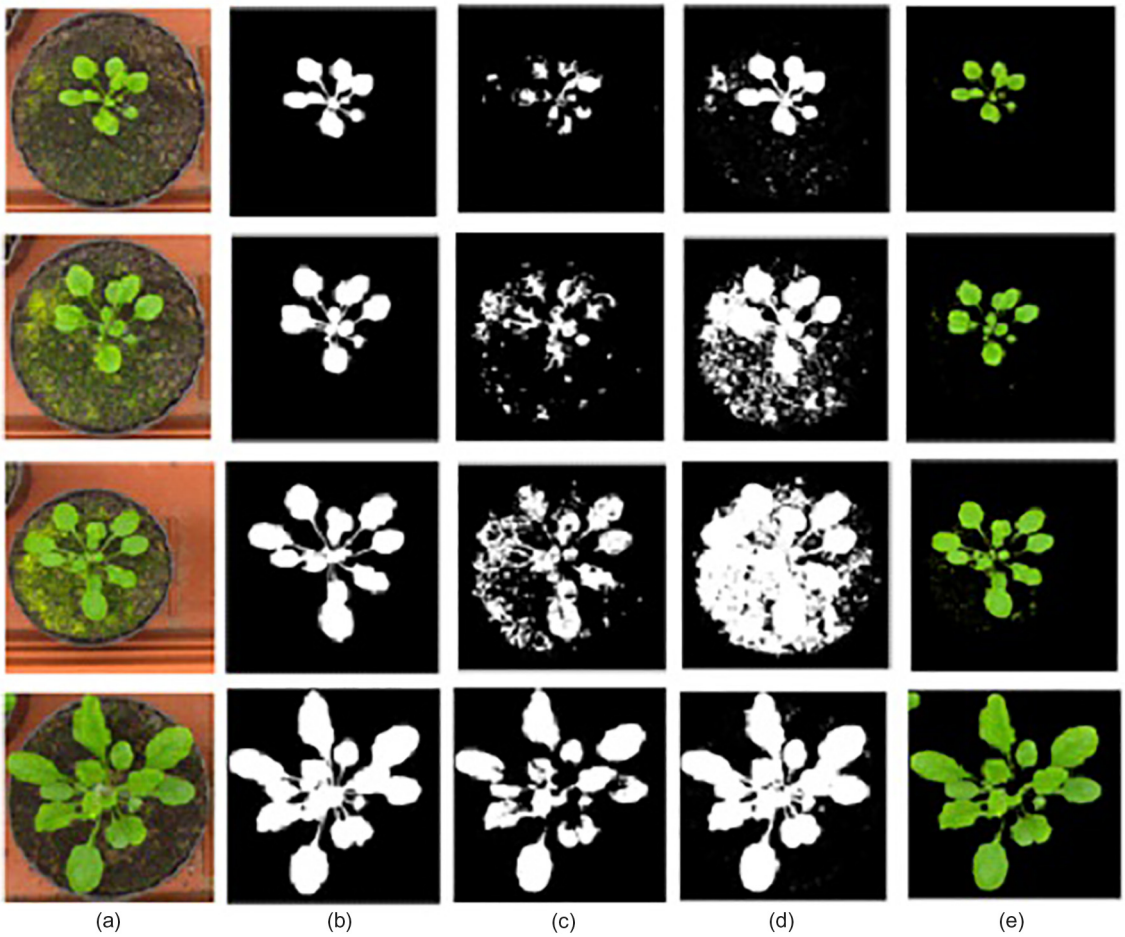

Fig. 12 – Leaf region extraction of individual plant images using various methods and tools. (a) Original image, (b) Ground truth, (c) Rosette Tracker (2012), (d) Reference method (2010), (e) Proposed method.

better than SLIC_Seg method. The proposed method achieves the leaf region extraction accuracy of 93.88% for the tray plant images which is higher than the existing tools and methods. Overall, the accuracy (Dice- 95.4%) of leaf region extraction for the datasets A1, A2 and A3, using our proposed method, is higher than SLIC_Seg method. In the proposed method, the standard deviation (shown in bracket) for leaf region extraction (FBD %) is less and the standard deviations (shown in bracket) for leaf count (DiC and |DiC|) are competitive, when compared with other method. This implies that the proposed method performs well equally for many plant images and thus maintains the robustness of the system.

The proposed method is also compared with various existing segmentation algorithms such as segmentation using contour detection and Hierarchical Image Segmentation (gPb-owt-ucm) [14], Saliency detection method by combining simple priors (SDSP) [29] and Co-segmentation via submodular optimization on anisotropic diffusion (CoSand) [28]. The figures (Fig. 11 and Fig. 12) show that the accuracy of extracting the leaf region by the proposed method is higher than the other segmentation methods applied in plant phenotyping to extract the leaf region. Fig. 13 shows the comparison of results of the proposed method with the plant phenotyping tool 'Rosette Tracker'. It is observed from Fig. 12 that the extraction of leaf region using Reference method [30] results in over segmentation and the extraction of leaf region using Rosette Tracker results in under segmentation. The accuracy of the proposed method to extract leaf region is closer to the ground truth.

The proposed method is also visually compared with the recent method [16] which is shown in Fig. 14. It is observed from Fig. 14 that the extraction of leaf region using the proposed method is similar to that of the method used in the paper [16]. The advantages of the proposed method over that of the method used in paper [16] are that the proposed method is independent of the camera used to capture the images and independent of the software used to preprocess the captured images, whereas the method used in paper [16] needs corresponding preprocessing software of the camera used to capture the images.

4. Conclusion

A new method with image enhancement technique and graph model for plant image segmentation and leaf counting is proposed. This method relies on the brightness distribution, graph algorithm, colour features and Circular Hough Transform. The experimentations are carried out and evaluated with image enhancement technique, as well as without using image enhancement technique. The proposed method is compared with existing tools and methods. The proposed method achieves the FBD of 95.4% (for datasets A1, A2, A3), which is higher than the SLIC_Seg method and it also achieves the Dice score of 93.88% (for tray plant images), which is higher than the existing methods or tools. The proposed method can be generally used to extract the leaf region not only in rosette plants, but also in all plants having green leaves. Leaf counting procedure can be applicable to all the

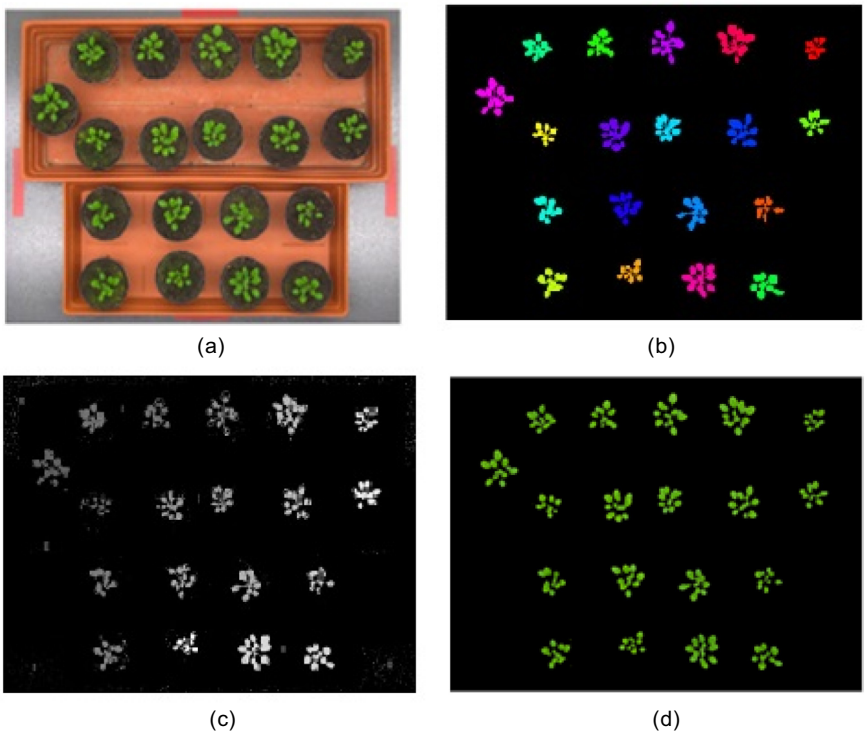

Fig. 13 – Leaf region extraction from tray plant images using various methods and tool. (a) Original image, (b) Ground truth, (c) Rosette Tracker (2012), (d) Proposed method.

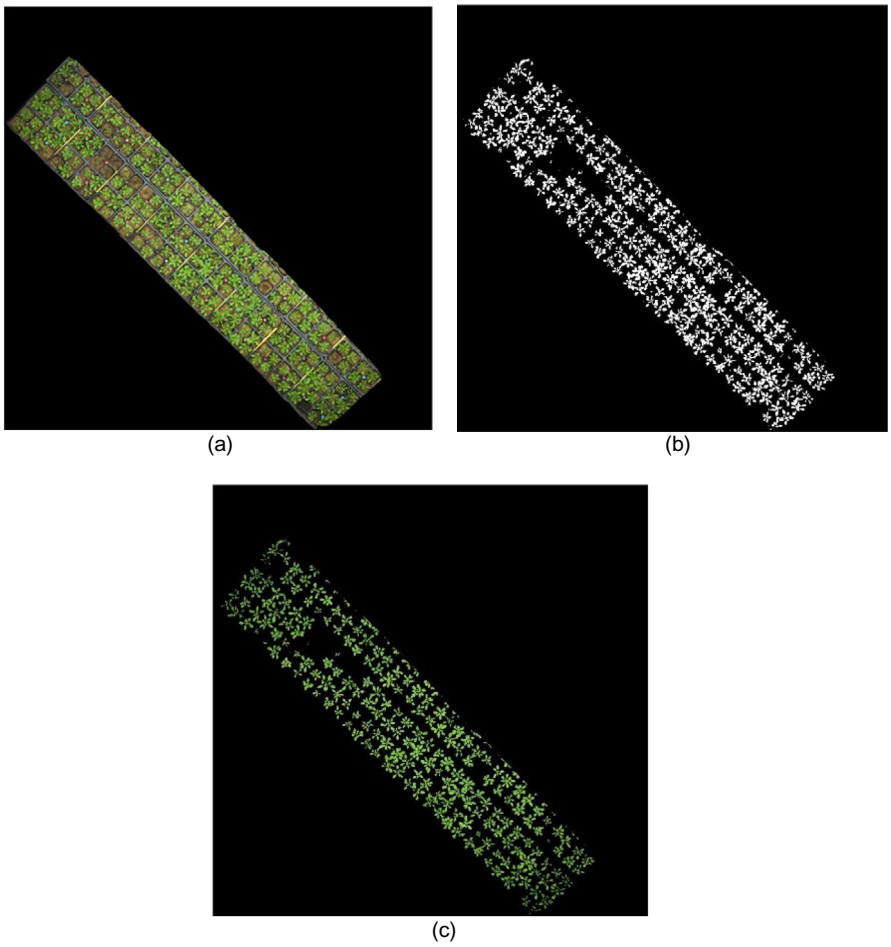

Fig. 14 – Leaf region extraction of plant image. (a) Original image, (b) Segmented binary image using method in [16] (c) Segmented color image using proposed method.

plants having elliptical or round shaped leaves. When the leaves are round in shape and green in colour, the efficiency of the proposed method will show dramatic increase in extracting the leaf region and counting the leaves. To increase the usage of this proposed method in plant phenotyping in future, this proposed method will be converted as an open source.

Conflict of interest

The authors declare that there is no conflicts of interest.

Acknowledgment

This research did not receive any specific grant from funding agencies in the public, commercial, or not-for-profit sectors.

REFERENCES

[1] Minervini M, Fischbach A, Scharr H, Tsaftaris SA. Finely-grained annotated datasets for image-based plant phenotyping. Pattern Recogn Lett 2016;81:80–9.

[2] Lobet G, Draye X, Périlleux C. An online database for plant image analysis software tools. Plant Methods 2013;9(38):1–7.

[3] Scharr H, Minervini M, French AP, Klukas C, Kramer DM, Liu XM, et al. Leaf segmentation in plant phenotyping: a collation study. Mach Vision Appl 2016;27(4):585–606.

[4] Huang YJ, Lee FF. An automatic machine vision-guided grasping system for phalaenopsis tissue culture plantlets. Comput Electron Agric 2010;70:42–51.

[5] Brochier MG, Vacavant A, Cerutti G, Kurtz C, Weber J, Tougne L. Tree leaves extraction in natural images: comparative study of preprocessing tools and segmentation methods. IEEE Trans Image Process 2015;24(5):1549–60.

[6] Tang X, Liu M, Zhao H, Tao W. Leaf extraction from complicated background. In: Proc CISP '09 Proceedings of the 2009 International Congress on Image and Signal Processing. Tianjin, China; 2009. p. 1–5.

[7] Chene Y, Rousseau D, Lucidarme P, Bertheloot J, Caffier V, Morel P, et al. On the use of depth camera for 3D phenotyping of entire plants. Comput Electron Agric 2012;82:122–7.

[8] Yin X, Liu X, Chen J, Kramer DM. Multi-leaf tracking from fluorescence plant videos. In: Proc ICIP '14 Proceedings of the 2014 IEEE international conference on image processing. Paris, France; 2014. p. 408–12.

[9] Dellen B, Scharr H, Torras C. Growth signatures of rosette plants from time-lapse video. IEEE/ACM Trans Comput Biol Bioinf 2015;12(6):1470–8.

[10] DeVylder J, Ochoa D, Philips W, Chaerle L, VanDerStraeten D. Leaf segmentation and tracking using probabilistic

parametric active contours. In: Proc. MIRAGE '11 Proceedings of the 2011 International Conference on Computer Vision/ Computer Graphics Collaboration Techniques. Rocquencourt, France; 2011. p. 75–85.
[11] Shen WZ, Zhang CL, Chen ZL. Research on automatic counting soybean leaf aphids system based on computer vision technology. In: Proc. ICMLC '07 Proceedings of the 2007 International Conference on Machine Learning and Cybernetics. Hong Kong, China; 2007. p. 1635–38.
[12] Cerutti G, Tougne L, Vacavant A, Coquin D. A parametric active polygon for leaf segmentation and shape estimation. In: Proc. ISVC '11 Proceedings of the 2011 International Symposium on Visual Computing. Las Vegas, USA; 2011. p. 202–13.
[13] DeVylder J, Vandenbussche F, Hu Y, Philips W, VanDerStraeten D. Rosette tracker: an open source image analysis tool for automatic quantification of genotype effects. Plant Physiol. 2012;160(3):1149–59.
[14] Arbelaez P, Maire M, Fowlkes C, Malik J. Contour detection and hierarchical image segmentation. IEEE Trans Pattern Anal Mach Intell 2011;33(5):898–916.
[15] Ning J, Zhang L, Zhang D, Wu C. Interactive image segmentation by maximal similarity based region merging. Pattern Recogn 2010;43(2):445–56.
[16] An N, Palmer CM, Baker RL, Markelz RJC, Ta J, Covington MF, et al. Plant high-throughput phenotyping using photogrammetry and imaging techniques to measure leaf length and rosette area. Comput Electron Agric 2016;127:376–94.
[17] Toro CAO, Martín CG, Pedrero AG, Ruiz EM. Superpixel-based roughness measure for multispectral satellite image segmentation. Remote Sens 2015;7(11):14620–45.
[18] Wu CH, Chang HH. Superpixel-based image noise variance estimation with local statistical assessment. J Image Video 2015;38:1–12.
[19] Ganesan P, Rajini V, Sathish BS, Khamar Basha Shaik. HSV colour space based segmentation of region of interest in satellite images. In: Proc. ICCICCT '14 Proceedings of the 2014 International Conference on Control, Instrumentation, Communication and Computational Technologies. Kanyakumari, India; 2014. p. 101–105.
[20] Ojo JA, Solomon ID, Adeniran SA. Contrast enhancement algorithm for colour images. In: Proc. SAI '15 Proceedings of the 2015 Science and Information Conference. London, UK; 2015. p. 555–559.
[21] Amini Z, Rabbani H. Statistical modeling of retinal optical coherence tomography. IEEE Trans Med Imag 2016;35 (6):1544–54.
[22] Chang KT. Analysis of the Weibull distribution function. J Appl Mech 1982;49(2):450–1.
[23] Illingworth J, Kittler J. The adaptive hough transform. IEEE Trans Pattern Anal Mach Intell 1987;9(5):690–8.
[24] Rizon M, Yazid H, Saad P, Shakaff AYM, Saad AR, Sugisaka M, et al. Object detection using circular hough transform. Am J Appl Sci 2005;2(12):1606–9.
[25] Chung KL, Huang YH. A pruning-and-voting strategy to speed up the detection for lines, circles, and ellipses. J Inf Sci Eng 2008;24(2):503–20.
[26] Yang JF, Hao SS. Modified hough transforms for object feature extraction. J Inf Sci Eng 2001;17(1):133–45.
[27] Canny J. A computational approach to edge detection. IEEE Trans Pattern Anal Mach Intell 1986;8(6):679–98.
[28] Kim G, Xing EP, Fei-Fei L, Kanade T. Distributed cosegmentation via submodular optimization on anisotropic diffusion. In: Proc. ICCV '11 Proceedings of the 2011 IEEE International Conference on Computer Vision. Barcelona, Spain; 2011. p. 169–76.
[29] Zhang L, Gu Z, Li H. SDSP: a novel saliency detection method by combining simple priors. In: Proc. ICIP '13 Proceedings of the 2013 IEEE International Conference on Image Processing. Melbourne, Australia; 2013. p. 171–75.
[30] Minervini M, Abdelsamea MM, Tsaftaris SA. Image-based plant phenotyping with incremental learning and active contours. Ecol Inform 2014;23:35–48.